Chapter 4 Influences of Compositional, Structural and Environmental Factors on

Soil EM Properties

4. 1 Introduction

The measured soil electromagnetic properties can be affected by a large number of factors as listed in Figure 4.1. This chapter focuses on studying the effects of soil compositional, structural and environmental factors on soil electromagnetic properties using the theoretical model developed in the previous chapter. The influences of measuring systems will be discussed in the next chapter. The effects of such factors as anisotropy, pore fluid salt concentration, clay mineralogy, clay percentage, water content and temperature are considered. Three theoretical correlations will be established for soils of different compositions: (1) correlation between volumetric water content and the real permittivity at 1 GHz, (2) correlation between volumetric water content and the dielectric dispersion magnitude from 50 MHz to 1 GHz, and (3) correlation between pore fluid electrical conductivity and soil bulk electrical conductivity at 20 MHz and 1 kHz. The strength of these correlations is evaluated by measuring the electromagnetic properties of saturated silicon sand, kaolinite, bentonite and mixtures of bentonite and silicon flour using a network analyzer.

```
┌─────────────────────────────────────┐
│ Applied Electrical Field            │
│                                     │
│  ● Frequency                        │
│                                     │
│  ● Magnitude                        │
└─────────────────────────────────────┘

┌─────────────────────────────────────┐
│ Soil Composition                    │
│                                     │
│  ● Clay mineralogy, clay percentage │
│                                     │
│  ● Gradation                        │
│                                     │
│  ● Water content                    │
│                                     │
│  ● Pore fluid chemistry             │
│                                     │
│  ● Degree of saturation             │
└─────────────────────────────────────┘

┌─────────────────────────────────────┐
│ Soil Microstructure                 │
│                                     │
│  ● Pore connection and tortuosity   │
│                                     │
│  ● Anisotropy                       │
│                                     │
│  ● Flocculation/dispersion          │
└─────────────────────────────────────┘

┌─────────────────────────────────────┐
│ Instrumental Factors                │
│  ● Probe electrode polarization     │
│                                     │
│  ● Skin (penetration) depth         │
└─────────────────────────────────────┘
```

Measured responses of a soil to the applied electromagnetic field

Figure 4.1 Factors that determine the measured soil electromagnetic properties

4.2 Effects of Various Factors on Soil EM Properties

The factors investigated in this chapter include the anisotropy, pore fluid salt concentration, state of dispersion and flocculation, volumetric water content, clay mineralogy, clay percentage, and temperature. To verify the results from the theoretical analysis, the equivalent dielectric permittivities of saturated silicon sand, kaolinite, Na-bentonite, Ca-bentonite and mixtures of Na-bentonite and silicon flour were measured. All measurements cited in this chapter were performed using a Hewlett-Packard HP-8752A impedance analyzer over the frequency range from 20 MHz to 1.3 GHz, except

for the the saturated Ca-bentonite, which was measured by Rinaldi and Francisca (1999) using a Hewlett-Packard HP4191A impedance analyzer over the frequency range from 1 MHz to 1 GHz.

The compositional parameters of the saturated kaolinite, sodium bentonite and calcium bentonite were back calculated by fitting the theoretical model proposed in Chapter 3 to the measured dielectric spectra of these soils. The compositional parameters and some physical properties of these soils are listed in Table 4.1. The sodium bentonite (SW 101 from WYO-BEN Inc) is a soil with a high percentage of smectite minerals. The kaolinite is a water-washed and air dried kaolin from Imerys, GA (Hydrite Flat D). The silicon flour was obtained by crushing silicon sand (Sil Co Sil 106). It was used in this study to make bentonite-silicon flour mixtures. The shape factor R of the silicon flour is assumed to be 1 because it has a high sphericity of 0.9.

Table 4.1 Some physical properties and optimized compositional parameters of the mixtures being studied

Soil	Physical properties				Compositional parameters		
	Total specific surface area, S_a (m^2/g)	Liquid limit (%)	Plastic limit (%)	Specific gravity	σ_{el} (S/m)	λ_s (S)	R
Na-bentonite	670	840	170	2.72	0.014	8.7×10^{-9}	161
Ca-bentonite	780 (estimated)	250	50	2.65	0.031	7.6×10^{-9}	62
Kaolinite	35	37	15	2.65	0.044	1.1×10^{-9}	3
Silicon flour*	0.113	-	-	2.65	-	0	1

* data provided by Prof. Santamarina of Georgia Tech

The saturated Ca-bentonite is used as a reference material to investigate the effects of pore fluid salt concentration and anisotropy for three reasons: (1) a small amount of bentonite can significantly change the electromagnetic property of a soil; (2) the smectite

minerals (major component of the bentonite) are sensitive to changes in pore fluid salt concentration; (3) the smectite particles form aggregates in the presence of Ca^+, which can be simulated by the theoretical model.

4.2.1 Effects of anisotropy

At high porosities, clay aggregates in a clay-water mixture are likely to be randomly oriented to form an isotropic mixture. The Ca-bentonite-water mixture tested by Rinaldi and Francisca (1999) had a very high volumetric water content of 0.89 (corresponding a void ratio of 8). Thus, all smectite aggregates in the mixture were assumed to be randomly oriented when the theoretical model was fitted to the measured dielectric spectrum to determine the compositional parameters in the previous chapter. Simplification has been made in the optimization as discussed previously in that the short major axes of the aggregates were equally divided into three portions: one portion in the XZ plane, one portion in the YZ plane and the other portion in the XY plane. The optimized compositional parameters are listed in Table 4.1.

Under the pressure in the vertical direction, the clay aggregates have a tendency to rotate towards the horizontal plane, leading to an anisotropic mixture. However, extreme anisotropy where all clay aggregates are parallel to the horizontal plane are unlikely for the saturated bentonite at high porosities because the behavior of smectite particles is primarily controlled by surface forces instead of body forces due to their high specific surface area. A small degree of anisotropy is possible and its influences on the dielectric spectrum of the saturated Ca-bentonite can be investigated by assuming that no aggregates have their short major axes oriented in the XY plane because the faces of the

clay particles in these aggregates are all perpendicular to the horizontal plane and they are

most likely to rotate towards the horizontal plane under vertical pressure as illustrated in

Figure 4.2.
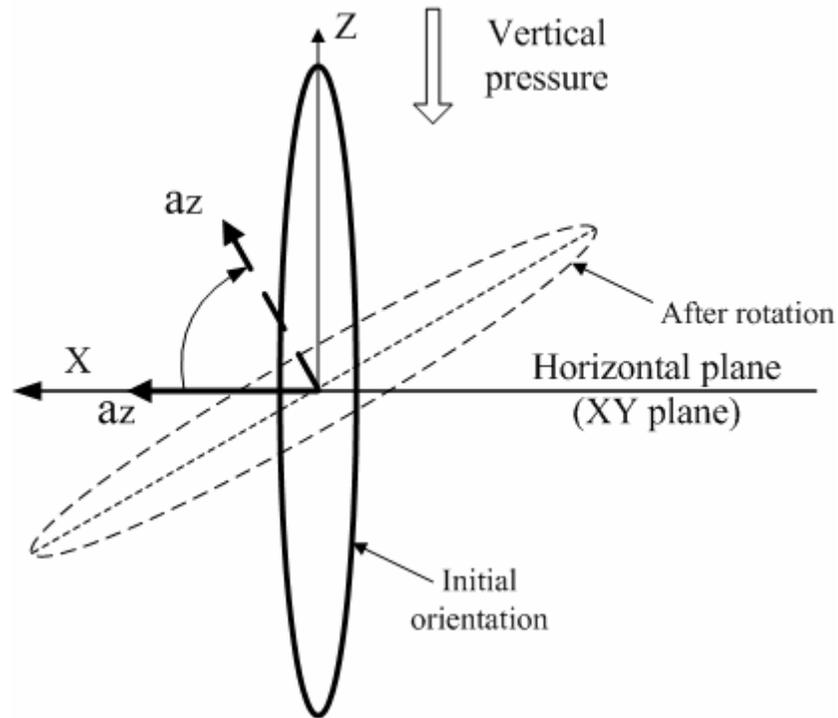
Figure 4.2 Vertically oriented aggregates tend to rotate under vertical pressure

The short major axes in the XZ and YZ planes are still assumed to be evenly

distributed, which leads to a case where one half of the short major axes are distributed in

the XZ plane and the other half in the YZ plane. The equivalent dielectric permittivities

of such a mixture are calculated for the vertical and horizontal directions and plotted in

Figure 4.3. A volumetric water content of 0.89 was assumed in the calculation and the

compositional parameters are from Table 4.1.
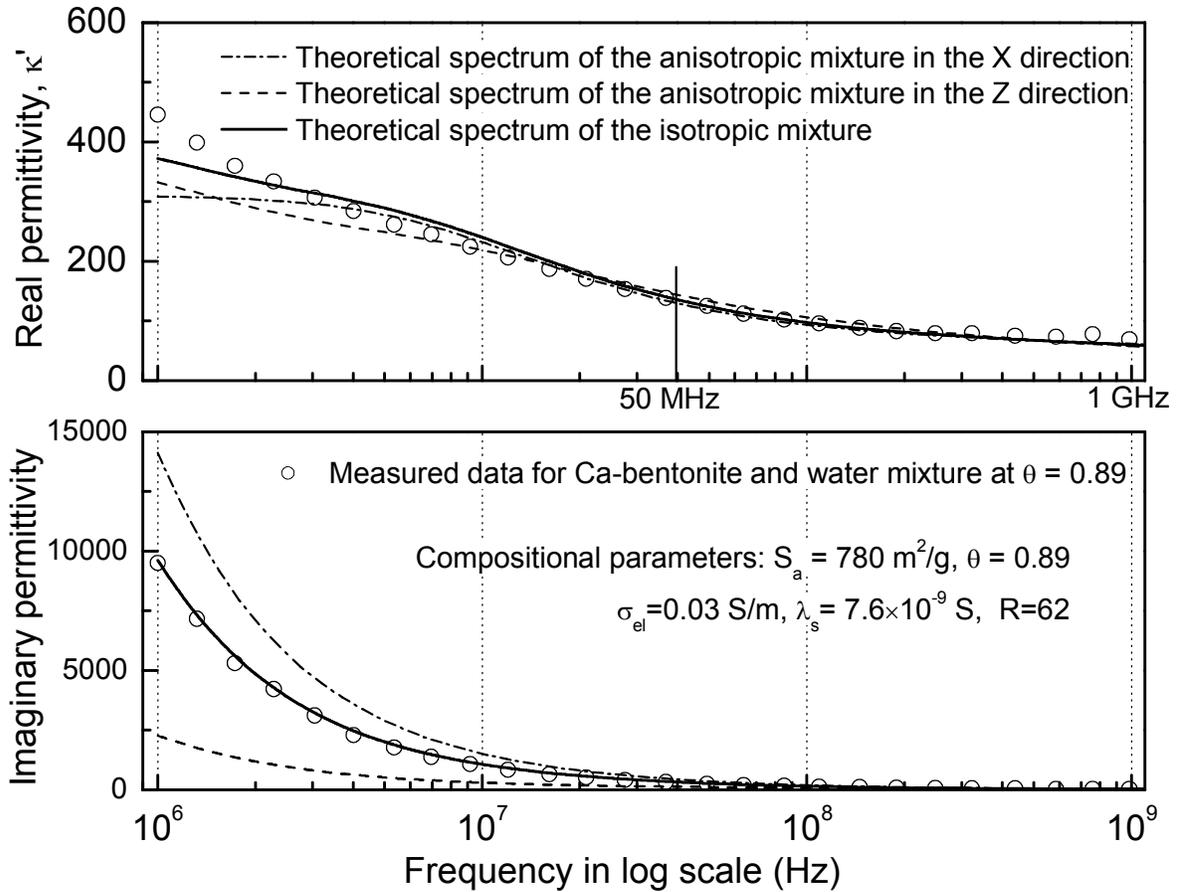
Figure 4.3 Effects of anisotropy on the dielectric spectrum of the saturated bentonite

The upper plot of Figure 4.3 shows the anisotropy only has a small impact on the dielectric dispersion curve (real permittivity as a function of frequency), especially at frequencies higher than 50 MHz. However, it has a big influence on the imaginary permittivity as shown in lower plot of Figure 4.3. An increase in anisotropy decreases the imaginary permittivity of the mixture in the Z direction and increases the imaginary permittivity of the mixture in the X direction because the contribution of surface conductance to the mixture DC electrical conductivity increases in the horizontal direction and decreases in the vertical direction when more clay aggregates are

horizontally oriented. The imaginary permittivity at low frequencies is controlled by the DC electrical conductivity of a soil. Significant changes in imaginary permittivity at low frequencies with increasing anisotropy indicate that the DC electrical conductivity might be a better indicator for anisotropy than the real permittivity for clayey soils.

4.2.2 Effects of pore fluid salt concentration

A change in the pore fluid salt concentration at first results in a change in the pore fluid DC electrical conductivity σ_{el}. The influences of pore fluid DC electrical conductivity σ_{el} on the dielectric spectrum of the saturated Ca-bentonite were investigated by varying the value of σ_{el} while keeping the values of all the other compositional parameters unchanged. The resulting dielectric spectra of the mixture are plotted in Figure 4.4.

It can be seen from the upper plot of the Figure 4.4 that at frequencies higher than 50 MHz, the dielectric dispersion curve is only slightly affected by the pore fluid DC electrical conductivity. At frequencies lower than 50 MHz, higher pore fluid DC electrical conductivities result in lower real permittivity. The physical reason for the decrease of mixture real permittivity with increasing pore fluid DC electrical conductivity is the suppression of interfacial polarization at lower frequencies. The interfacial polarization is the primary reason leading to the increase of mixture real permittivity at low frequencies. It is induced because the clay aggregates have a higher DC electrical conductivity than the bulk pore fluid when they are oriented parallel to the external EM field. This difference in DC electrical conductivity results in an accumulation of charges at the interfaces between clay aggregates and bulk pore fluid, which in turn increases the

polarizability of the mixture. When an increase in the pore fluid DC electrical

conductivity narrows this difference, the interfacial polarization is suppressed and the real

permittivity decreases accordingly. On the other hand, the imaginary permittivity

increases with increasing pore fluid DC electrical conductivity σ_{el} as shown in the lower

part of Figure 4.4 because a more conductive pore fluid results in a more conductive

mixture.
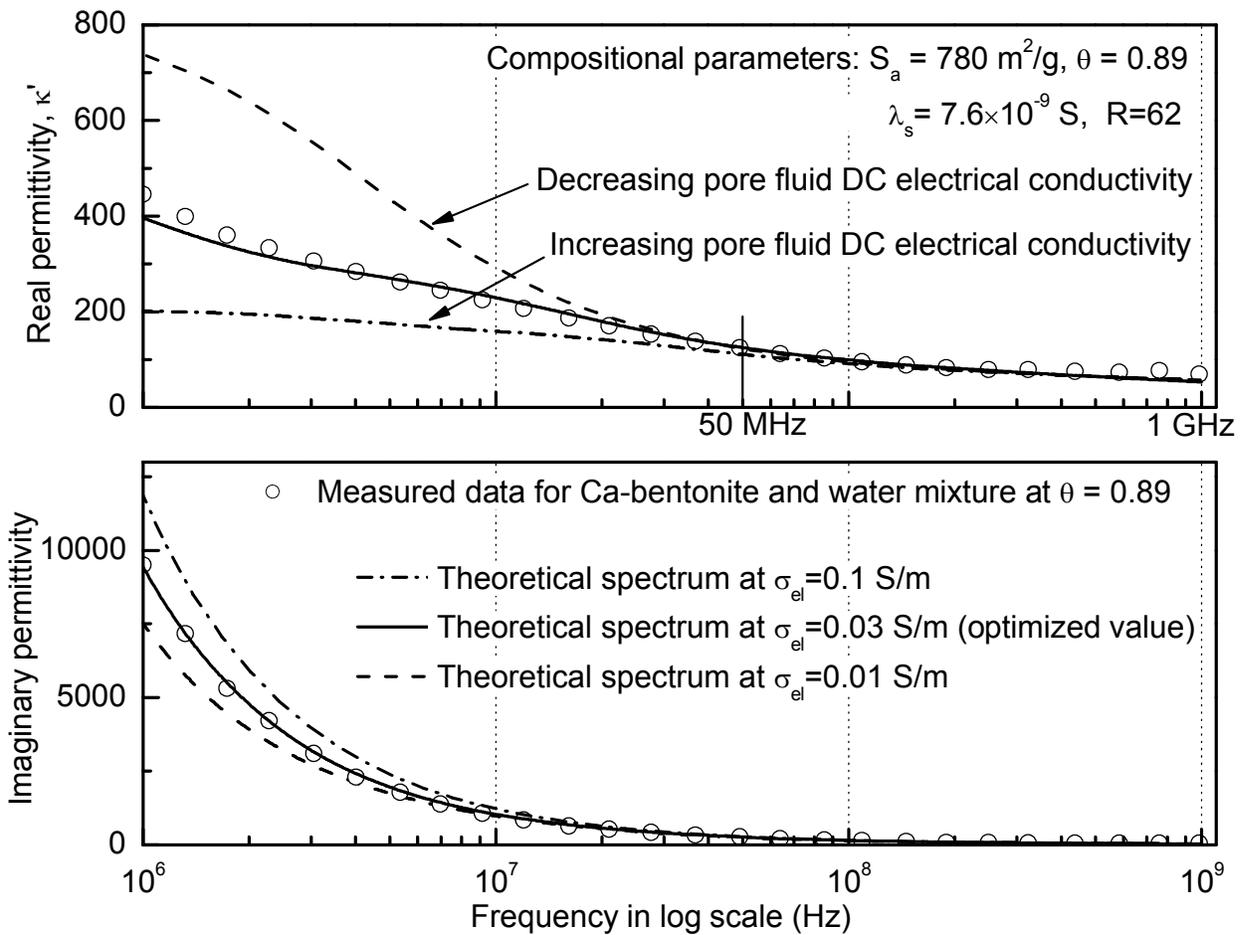
Figure 4.4 Effects of pore fluid electrical conductivity on the dielectric spectrum of the

Ca-bentonite-water mixture

4.2.3 Effect of dispersion and flocculation

Smectite and illite particles are usually dispersed in the bulk pore fluid when the counterions are Na^+ and the pore fluid salt concentration is low. The calculation for the equivalent dielectric permittivity of a soil containing dispersed clay particles is identical to that for a soil containing clay aggregates because the dispersed clay particles can be considered as special clay aggregates sandwiched by external bound water layers without internal water layers. For dispersed clay particles, the intra-aggregate pore fluid refers to the bound water layers attached to the external surfaces of clay particles.

One difference between the flocculated and dispersed states of dispersive soils is the shape of clay inclusions: the clay aggregates have larger thickness than but similar width as individual clay particles. Another difference is the amount of intra-aggregate pore fluid. When clay particles are totally dispersed, about three molecular layers of bound water are attached to each side of a dispersed clay particle and the average thickness of the intra-aggregate pore fluid t_w is approximately 18 Å because the thickness of each water molecular layer is about 3 Å. When clay particles form aggregates, the distance between two adjacent clay particles is approximately 9.5 Å, which is also the average thickness of the intra-aggregate pore fluid. Therefore, a shift from a dispersed state to a flocculated state corresponds to (1) a decrease in the shape factor R, which determines the ratio between the width and thickness of the clay inclusions; (2) a decrease in the average thickness of intra-aggregate pore fluid from 18 Å to 9.5 Å. The average dielectric permittivity of the intra-aggregate pore fluid is changed accordingly by changing the

value of *m* in equation [3.20] from 3 to 2 because the intra-aggregate pore fluid in an aggregate is affected by surface forces from two adjacent particles.

The saturated Na-bentonite at a volumetric water content of 0.924 is used as a reference material to study the effects of flocculation. The measured and optimized dielectric spectra of the saturated Na-bentonite are shown in Figure 4.5. The smectite particles were assumed to be totally dispersed and randomly oriented in the bulk pore fluid in the optimization. The compositional parameters that yield best fit for the measured dielectric spectrum are listed in Table 4.1.

Assume that the shape factor R decreases from 161 to 50 and the average thickness of the intra-aggregate pore fluid decreases from 18 Å to 9.5 Å when the sodium counterions are substituted by calcium counterions. The optimized values of the other compositional parameters are unchanged. The resulting equivalent dielectric permittivity of the mixture is plotted in Figure 4.5. It can be seen that the real permittivity of the mixture increases over the entire frequency range: the lower the frequency, the higher the magnitude of increase. On the other hand, the imaginary permittivity of the mixture decreases with flocculation.

The state of dispersion and flocculation can also be affected by the salt concentration. The clay aggregates tend to get further flocculated with increasing salt concentration because the thickness of the diffuse double layer is suppressed and the repulsive forces between clay particles become smaller (Mitchell 1993). Therefore, the clay aggregates become thicker and the shape factor R becomes even smaller. To simulate this situation, the shape factor R is at first decreased to 25 without changing other compositional factors. It can be seen from Figure 4.5 that the flocculation causes a further increase in the

mixture real permittivity and further decrease in the mixture imaginary permittivity. However, a higher salt concentration also results in a higher pore fluid DC electrical conductivity. Therefore, the pore fluid DC electrical conductivity is increased ten times from 0.014 S/m to 0.14 S/m, to investigate the changes of the mixtures equivalent dielectric permittivity when the flocculation and increasing pore fluid DC electrical conductivity take place at the same time. Figure 4.5 shows that the effects of flocculation and increasing pore fluid DC electrical conductivity tend to cancel each other and the resulting dielectric spectrum is close to the one before the increase of pore fluid salt concentration. Therefore, the actual influences of salt concentration on the EM properties of a soil may be less pronounced than predicted in Figure 4.4 when the flocculation occurs, because the flocculation tends to compensate for the influences of increasing pore fluid DC electrical conductivity.
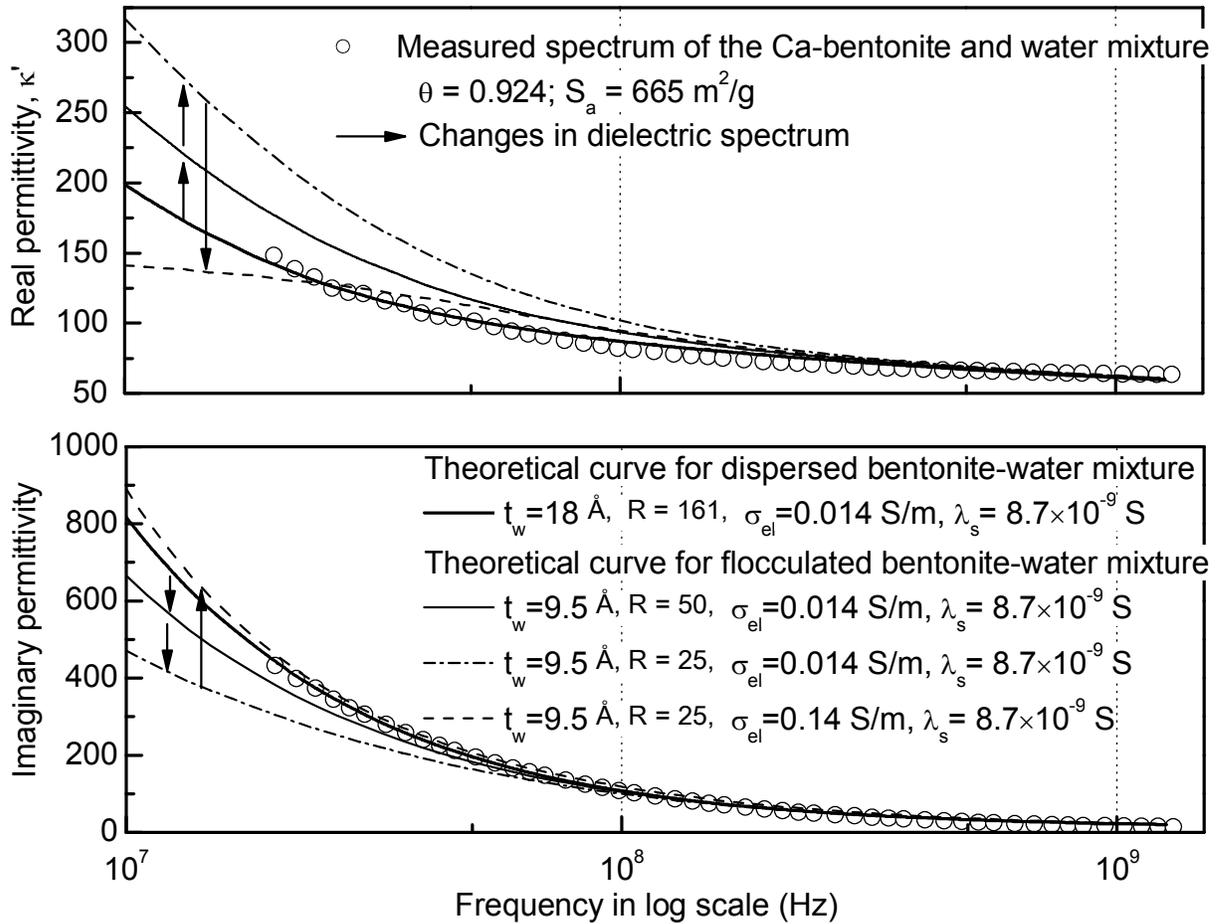
Figure 4.5 Effects of dispersion and flocculation on the dielectric spectrum of bentonite-water mixture

4.2.4 Effects of volumetric water content and clay mineralogy

Effects of volumetric water content on the dielectric spectrum are investigated by changing the overall porosities of the saturated Na-bentonite and kaolinite while keeping the values of the compositional parameters from Table 4.1 unchanged. The theoretical dielectric spectra of the saturated Na-bentonite at four volumetric water contents θ = 0.9, 0.93, 0.96 and 0.99 are plotted in Figure 4.6. The theoretical dielectric spectra of the saturated kaolinite at four volumetric water contents θ = 0.5, 0.55, 0.60 and 0.65 are

plotted in Figure 4.7.The optimized compositional parameters used in calculation are also shown in the two figures.

To validate the theoretical dielectric spectra, the equivalent dielectric permittivities of the saturated Na-bentonite at three volumetric water contents $\theta = 0.937$, 0.944 and 0.954 were measured and plotted in Figure 4.6. The equivalent dielectric permittivities of the saturated kaolinite at three volumetric water contents $\theta = 0.57$, 0.60 and 0.63 were also measured and plotted in Figure 4.7.

Figure 4.6 shows that the measured dielectric spectra of the saturated Na-bentonite at $\theta = 0.937$ and 0.954 are very close to the predicted dielectric spectra at $\theta = 0.93$ and 0.96. The measured and predicted dielectric spectra of the kaolinite at $\theta = 0.60$ agrees very well. In general, the theory well predicted the measured changes in equivalent dielectric permittivity with volumetric water content.

The upper plot of Figure 4.6 shows that the real permittivity of the saturated Na-bentonite decreases at high frequencies but increases at low frequencies with decreasing volumetric water content, and the dielectric dispersion curves converge at a frequency of about 100 MHz. An increase in the mixture real permittivity at low frequencies with decreasing volumetric water content is most likely due to interfacial polarization, which is very strong for the saturated bentonite because the bentonite has a very high total specific surface area (665 m^2/g) and a high surface conductance ($\sim 8.7 \times 10^{-9}$ S), which in turn lead to a very high DC electrical conductivity of bentonite particles when the bentonite particles are oriented parallel to the external EM field (as high as 5 S/m). The big difference between the bentonite particles and bulk pore fluids in DC electrical conductivity induces strong interfacial polarization and a higher volumetric fraction of

113

bentonite particles further enhances this impact of interfacial polarization at low frequencies. Thus an increase in the mixture real permittivity with decreasing volumetric water content is observed. At high frequencies where the effects of interfacial polarization become small, the amount of bulk pore fluid controls the mixture real permittivity because the bulk pore fluid has a much higher real permittivity (about 79 at frequencies lower than 1 GHz) than the solid clay particles (about 5). Thus, the mixture real permittivity decreases with decreasing volumetric water content.

The lower plot of Figure 4.6 shows that the mixture imaginary permittivity increases with decreasing volumetric water content. This is because a decreasing volumetric water content leads to a higher volumetric fraction of bentonite particles with high surface conductance, which in turn makes the mixture more conductive.

The saturated kaolinite exhibits different behavior from the saturated bentonite. The upper plot of Figure 4.7 shows that the dielectric dispersion curves decrease almost parallelly with decreasing volumetric water content over the entire frequency range. The dielectric dispersion magnitude is small because both the specific surface area and surface conductance of kaolinite minerals are small and the effects of interfacial polarization are not strong. Thus, the amount of bulk pore fluid is the most important factor controlling the real permittivity of the saturated kaolinite.

The imaginary permittivity of the saturated kaolinite is almost unchanged with decreasing volumetric water content because the contributions of pore fluid electrical conductivity and kaolinite surface conductance to the mixture electrical conductivity are almost equal at this specific pore fluid salt concentration. At other pore fluid salt

concentrations, the imaginary permittivity will change with changing volumetric water content.

The differences between the bentonite and kaolinite dielectric spectra demonstrate that both volumetric water content and clay mineralogy play important roles in determining the dielectric spectrum of a soil. How the volumetric water content and clay mineralogy affect the real and imaginary permittivities will be further discussed in the following sections.
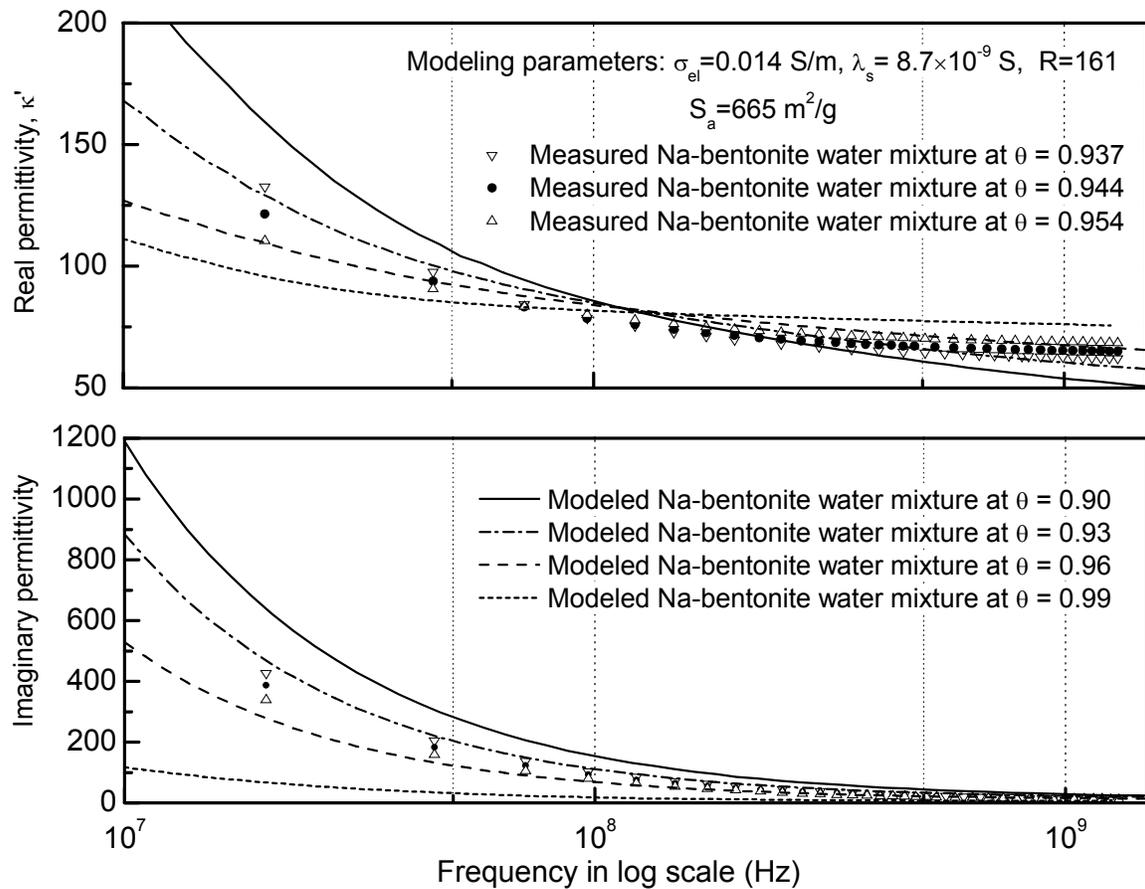

Figure 4.6 Effects of volumetric water content on the dielectric spectrum of the saturated Na-bentonite
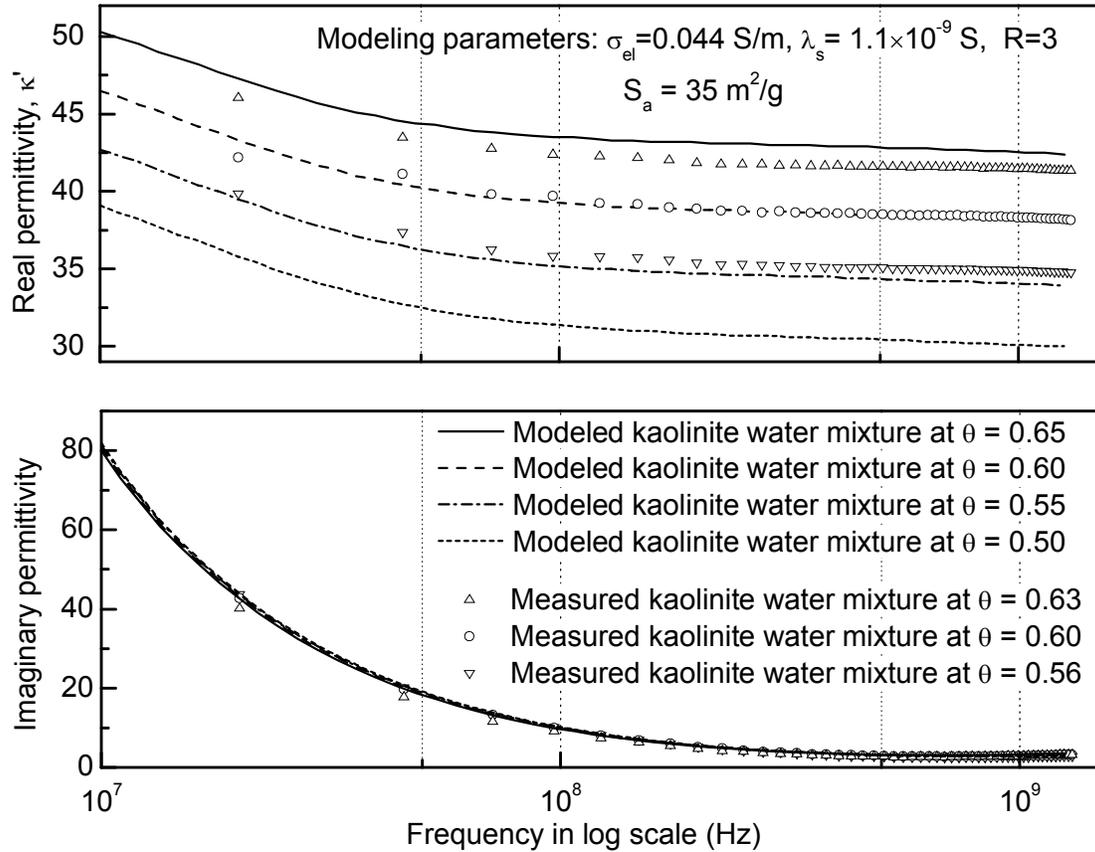
Figure 4.7 Effects of volumetric water content on dielectric spectrum of the saturated kaolinite

4.2.5 Effect of clay percentage

To investigate the effects of clay percentage on dielectric spectra of soils, mixtures of Na-bentonite and silicon flour were prepared by at first mixing the Na-bentonite with deionized water to a volumetric water content of 0.928 and then adding different amounts of dry silicon flour to the bentonite-water mixture. Six samples were prepared and the ratios between the dry weight of silicon flour and Na-bentonite in these samples are 0, 1, 2, 4, 8 and 16, respectively. Since the specific gravities of the silicon flour and Na-bentonite are very close (refer to Table 4.1), their volumetric ratios in these samples are

also approximately 0, 1, 2, 4, 8 and 16. When the weight of the silicon flour is 16 times that of bentonite, a small amount of deionized water was added to facilitate the mixing process because the sample was too dry to be thoroughly mixed. The equivalent dielectric permittivities of these samples were measured using the impedance analyzer, and the results are plotted in Figure 4.8. The gravimetric water contents were determined by oven drying the soil samples at 105 ºC and the volumetric water contents were calculated by assuming all solids in the mixtures have a specific gravity of 2.65.

Since the bentonite and silicon flours have been thoroughly mixed, the large silicon flour particles are assumed to be evenly distributed in the microfabric formed by the bentonite particles. Therefore, the saturated mixture of bentonite and silicon flour can be modeled by adding sand particles gradually to a bentonite-water mixture as if they were added to an electrolyte. At first, the equivalent dielectric permittivity of the saturated Na-bentonite is calculated using the theoretical model and the optimized compositional parameters listed in Table 4.1. Then the saturated bentonite is treated as a new medium for the addition of sand particles. The ratios between the volume of sand particles and that of Na-bentonite are assumed to be 0, 1, 2, 4, 8 and 16 and the overall volumetric water contents of the modeled mixtures are assumed to be the same as those of the tested samples. The theoretical dielectric spectra are also plotted in Figure 4.8. In the calculation, the sand particles are assumed to be spherical (shape factor R = 1) and nonconductive (surface conductance $\lambda_s = 0$). The dielectric permittivities of both sand and solid bentonite particles κ_s are assumed to be 5.

Figure 4.8 shows that the theoretical dielectric spectra match very well with the measured dielectric spectra at almost all combinations of bentonite and silicon flours.

117

Both the real and imaginary permittivities of the mixture decrease with increasing amount of silicon flour, which reflects the decrease of the volumetric water content. Moreover, the dielectric dispersion curve becomes flatter with increasing amount of silicon flour. Excellent matches between the theoretical and measured dielectric spectra demonstrate that the model is not only valid for saturated sand and pure clay but also valid for mixtures containing both clay and nonclay minerals. It may also be applicable for mixtures containing several clay minerals as long as no chemical reactions occur between them.
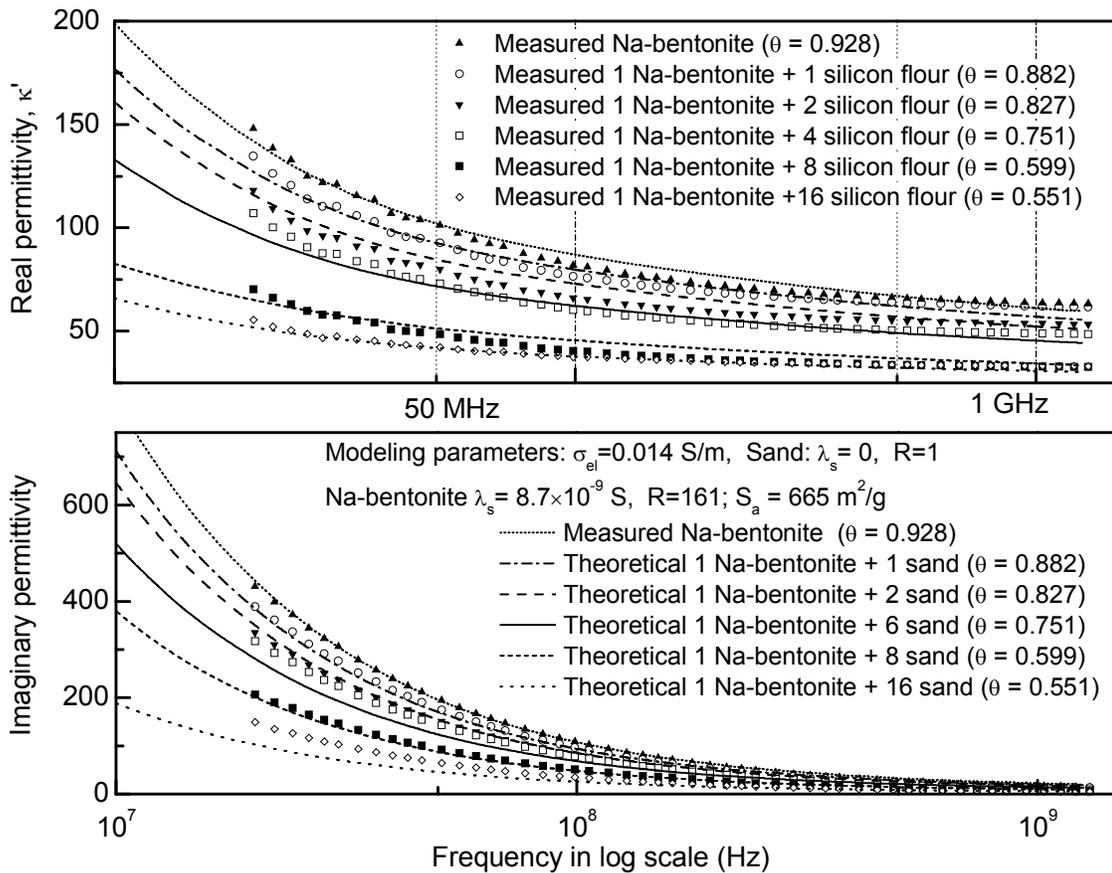
Figure 4.8 Measured and theoretical dielectric spectra of sand-clay-water mixtures

4.2.6 Effects of temperature

An increase in temperature will cause a series of changes in soil components and structure, for example, the surface conductance will increase, the thickness of bound water layer will decrease and the real permittivity of the bulk pore fluid will decrease. The surface conductance increases because the energy barrier in the Stern layer decreases with increasing temperature and the counterions have more freedom to move along clay surfaces. The changes in dielectric permittivity of bulk pore fluid with temperature are plotted in Figure 3.2 of the previous chapter.

The equivalent dielectric permittivities of the Canisteo clay loam were measured by Logsdon and Hornbuckle (2006) at three water contents and two temperatures. The dielectric spectra of the Canisteo clay loam are plotted on the left side of Figure 4.9. Since the mineralogical composition of the Canisteo clay loam is unknown, the theoretical dielectric spectrum of an imaginary mixture of illite and sand at similar temperatures and water contents as the Canisteo clay loam is studied. The surface conductance of illite is assumed to be 8×10^{-9} S/m at 25 ℃ and its shape factor R is assumed to be 10. The sand particles are assumed to be spherical (R=1) and non-conductive (λ_s=0). The pore fluid DC electrical conductivity is set to be 0.1 S/m. Assume that two changes occur when the temperature increases from 5 ℃ to 25 ℃: (1) the surface conductance of illite increases from 4×10^{-9} S/m to 8×10^{-9} S/m because the energy barrier preventing counterions to move drops with increasing temperature; (2) the pre-relaxation real permittivity of bulk pore fluid decreases from 85 to 79 and its relaxation frequency increases from 10 GHz to 18 GHz as shown in Figure 3.2. The

theoretical dielectric spectra for the saturated illite-sand mixture are plotted on the right

side of Figure 4.9.
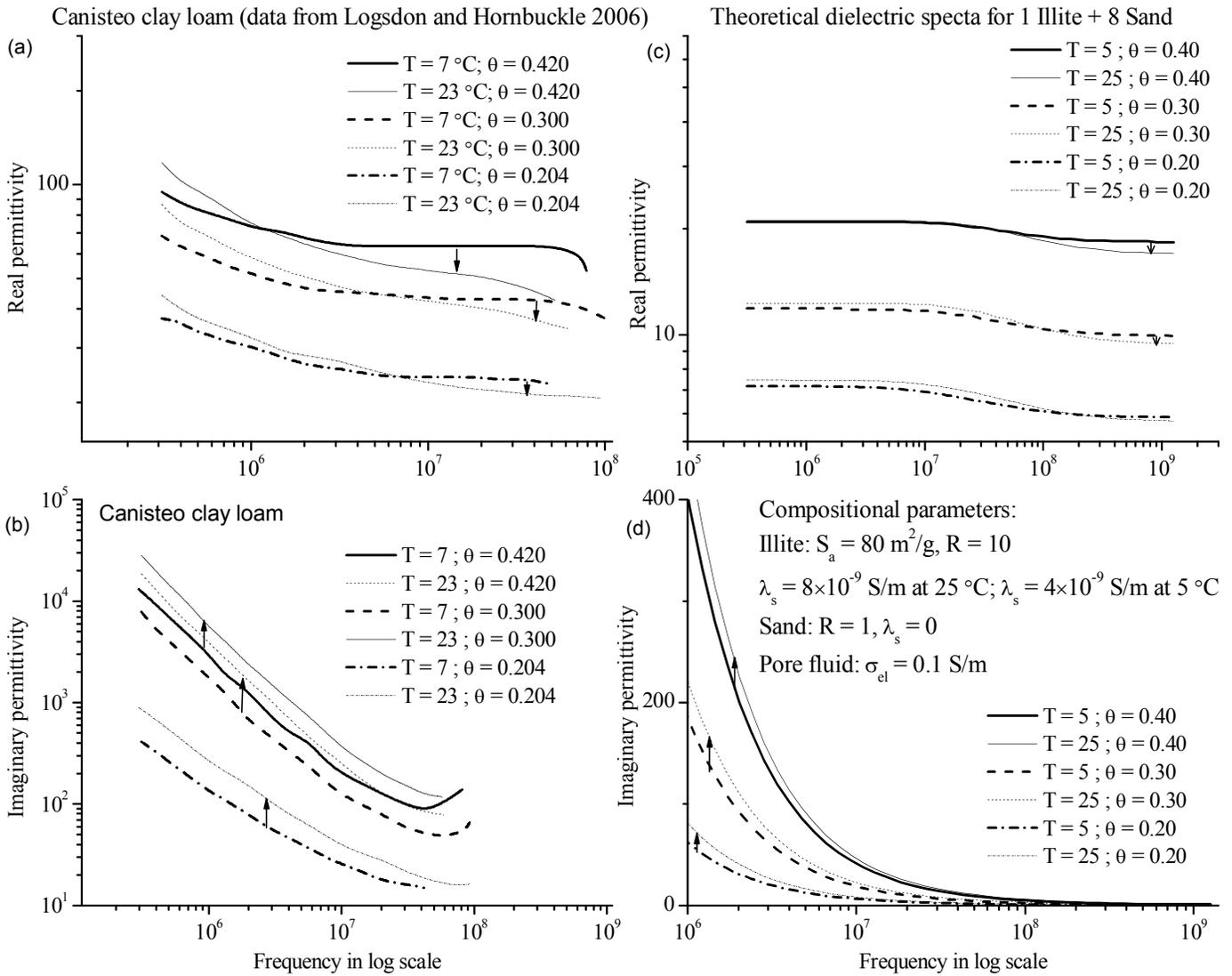
Figure 4.9 Effects of temperature on the dielectric spectra of Canisteo clay loam and an

imaginary mixture of illite and sand

It can be seen from Figure 4.9 that, although the changes in the magnitudes of real

and imaginary permittivities and the frequency where the changes occur are different for

the two soils, they exhibit exactly the same behavior with increasing temperature. The real permittivities decrease at high frequencies but increases at low frequencies; the imaginary permittivities increases over the entire frequency range regardless of the volumetric water content. These results suggest that a better understanding of the effects of temperature on soil properties may be achieved by studying the temperature-dependent electromagnetic properties of soils with known mineralogy.

4.3 Relationship between clay mineralogy, volumetric water content and real permittivity

The previous analyses show that pore fluid salt concentration, flocculation, anisotropy, volumetric water content, clay mineralogy and percentage of clay can affect the dielectric spectrum of a saturated clayey soil. However, at frequencies higher than 50 MHz, the influences of pore fluid chemistry and anisotropy on the dielectric dispersion curve of a soil become relatively small as shown in Figures 4.3 and 4.4. Over the 50 MHz and 1 GHz frequency range, factors controlling the dielectric dispersion curve are primarily the volumetric water content, clay type and clay percentage. It is of great practical significance to study how the real permittivity at 1 GHz and the decrease of the real permittivity from 50 MHz to 1 GHz (dielectric dispersion magnitude) are affected by volumetric water content, clay mineralogy and clay percentage because it might lead to simple methods to determine these fundamental properties from electromagnetic measurements. To that end, two sets of theoretical correlations were developed for saturated sand, kaolinite, Na-bentonite and mixtures of Na-bentonite and sands using the theoretical model and the compositional parameters listed in Table 4.1: (1) volumetric

121

water content and the real permittivity at 1 GHz and (2) volumetric water content and the dielectric dispersion magnitude from 50 MHz to 1 GHz. All soils are assumed to be isotropic in the calculation. The theoretical correlations for the saturated bentonite-sand mixtures were constructed by at first calculating the theoretical real permittivities of a saturated sodium bentonite at volumetric water contents from 0.7 to 0.99 and then adding different amount of sand particles to the bentonite-water mixture. The minimum volumetric water content of the saturated bentonite was set as 0.7 to ensure that at least three molecular layers of bound water are attached to each side of a clay particle, which gives a intra-aggregate volumetric water content of 0.66 for the sodium bentonite with a total specific surface area of 665 m^2/g. The theoretical correlations are plotted in Figure 4.10.

To evaluate the reasonableness of these theoretical correlations, the real permittivities at 1 GHz and dielectric dispersion magnitudes from 50 MHz to 1 GHz of the saturated silicon sand at two water contents, kaolinite at four water contents, Na-bentonite at four water contents and mixtures of Na-bentonite and silicon flour at different proportions were measured using the impedance analyzer. The experimental data are shown in Figure 4.10. It can be seen that almost all measured values are well predicted by the theoretical correlations.

The differences in theoretical correlations for different soils can be related to their differences in total specific surface area. The total specific surface area of a soil is defined as the total surface area a soil divided by its dry mass. The silicon flour is crushed silicon sand with a very low specific surface area (0.113 m^2/g) while the specific surface area of the Na-bentonite is very high (665 m^2/g). Therefore, when the silicon flour and

122

bentonite are mixed, the total surface area of the mixture is close to that of Na-bentonite but the total mass is increased. Therefore, the total specific surface area of a bentonite-silicon flour mixture decreases with increase of silicon flour. The total specific surface areas of the bentonite-silicon flour mixtures are approximately 333, 221, 133, 74 and 39 m^2/g when the weight ratios between the silicon flour and Na-bentonite are 1, 2, 4, 8 and 16, respectively. The total specific surface area of kaolinite is 35 m^2/g and that of silicon sand is less than 1 m^2/g. Therefore, a trend presented in Figure 4.10 is that the higher the specific surface area, the lower the real permittivity at 1 GHz and the higher the dielectric dispersion magnitude from 50 MHz to 1 GHz at the same volumetric water content.

The upper plot of Figure 4.10 shows that, for a specific soil, the real permittivity at 1 GHz decreases with decreasing volumetric water content. However, a high specific surface area soil has a much higher volumetric water content than a low specific surface area soil if the same real permittivity is measured at 1 GHz. The lower plot of Figure 4.10 shows that, for high specific surface area soils, the dielectric dispersion magnitude increases with decreasing volumetric water content. For soils with low to medium specific surface areas, the dielectric dispersion magnitude does not change much over a wide volumetric water content range. This indicates the dielectric dispersion curves of soils with low to medium specific surface areas will decrease almost parallelly with decreasing volumetric water content over the 50 MHz to 1 GHz frequency range. This tendency has been demonstrated by the dielectric dispersion curves of the saturated kaolinite in Figure 4.7.
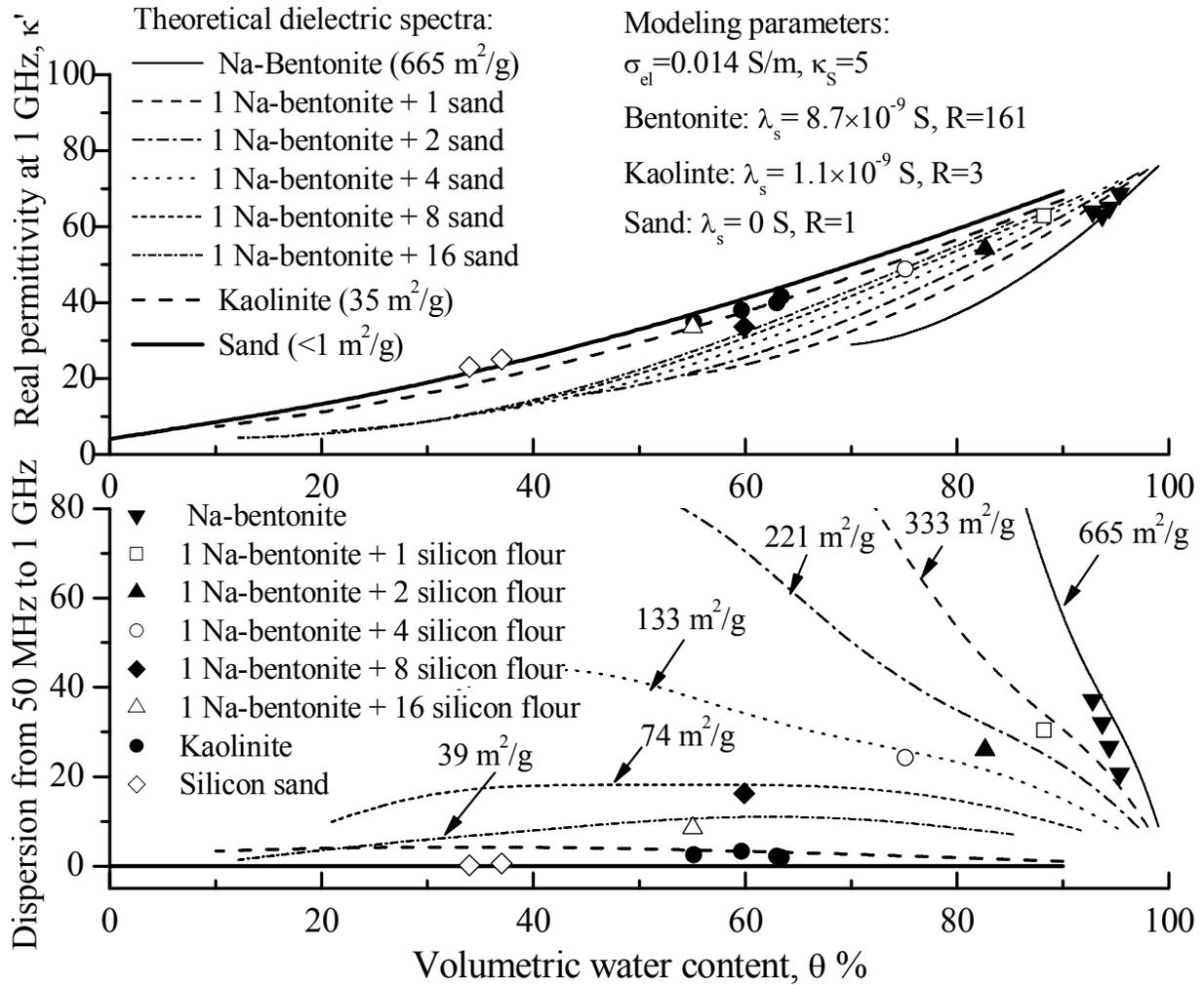
Figure 4.10 Theoretical correlations between the volumetric water content, real permittivity at 1 GHz and dielectric dispersion from 50 MHz to 1 GHz

The good matches between the theoretical correlations and experimental data in Figure 4.10 indicate that a simple method to determine the total specific surface area and volumetric water content can be developed by measuring the real permittivities at 50 MHz and 1 GHz. The procedure includes four steps and is illustrated in Figure 4.11 for an imaginary soil with a real permittivity of 90 at 50 MHz and 40 at 1 GHz. The dielectric dispersion magnitude $\Delta\kappa'$ of 50 is calculated as the difference between these

two permittivities. The first step is to determine the range of the volumetric water

contents from the real permittivity at 1 GHz by drawing a horizontal line that intersects

the theoretical correlations in the upper plot of Figure 4.11. The second step is to

determine the corresponding dielectric dispersion magnitudes for different soils in the

lower plot of Figure 4.11 at the porosities determined in the first step. The third step is to

connect these dielectric dispersion magnitudes with straight lines. The fourth step is to

draw another straight line through the dielectric dispersion magnitude at 50, which will

intersect the polyline drawn in the third step. From this intersection, the volumetric water

content of the soil is determined to be 0.73 and the total specific surface area of the soil is

estimated to be 260 m^2/g. This procedure is applicable for sand, silt, pure clay and

mixtures of sand and pure clay. Its applicability for natural soils in which a variety of

clay minerals coexist needs to be validated.
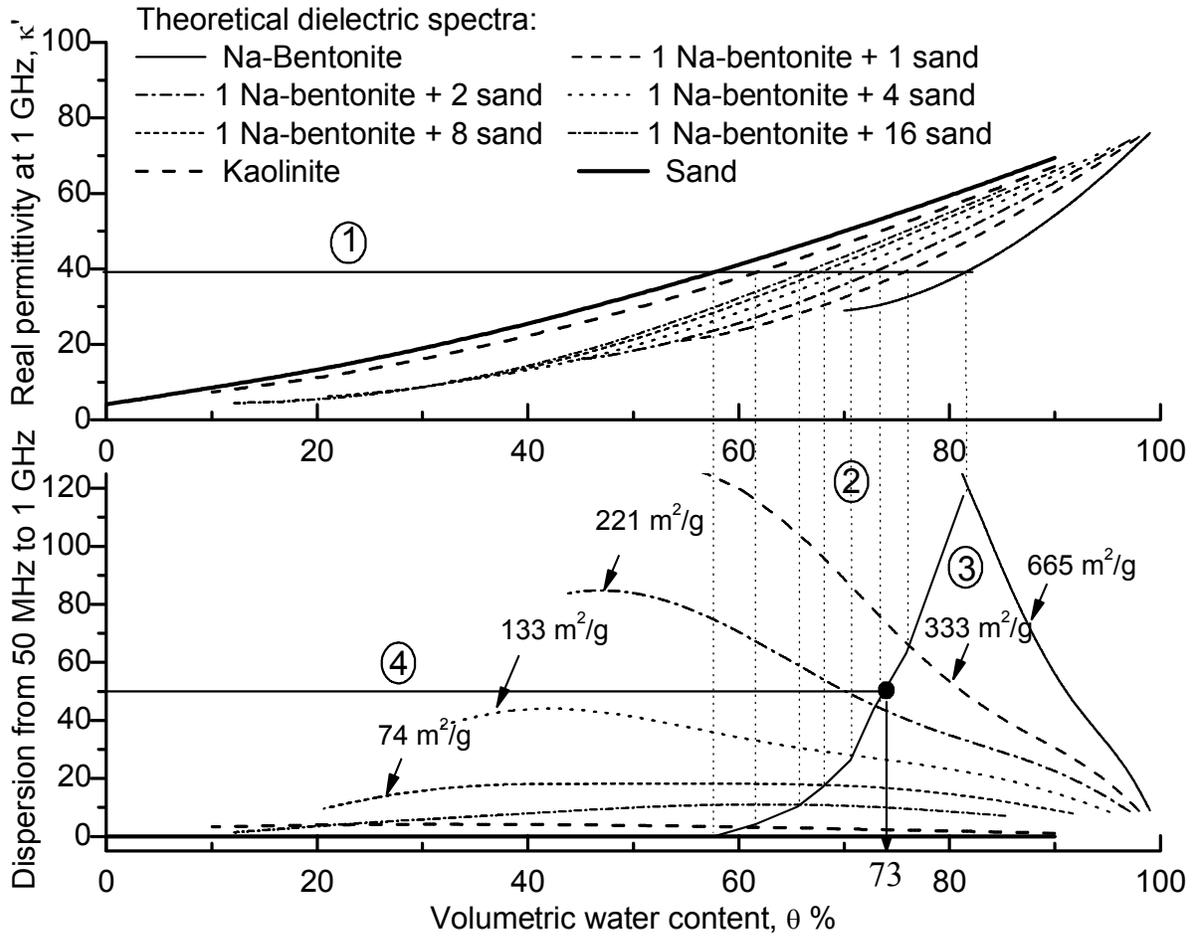
Figure 4.11 A simple method to determine the volumetric water content and total specific surface area

4.4 Relationship between clay mineralogy, volumetric water content and effective electrical conductivity

Clay percentage, clay mineralogy and volumetric water content also play important roles in determining the electrical conductivity of a soil. From the theoretical model, the relationships between the effective electrical conductivity and volumetric water content can also be developed for soils with different components. Theoretical correlations between the volumetric water content and effective electrical conductivity for saturated

bentonite-sand mixtures at different proportions are plotted in Figure 4.12. The effective

electrical conductivity is converted from the imaginary permittivity through equation

[2.2] and calculated at two frequencies: 20 MHz and 1 kHz. The theoretical correlations

at 20 MHz were computed so that the measured effective electrical conductivities of the

saturated Na-bentonite and silicon flour mixtures by the impedance analyzer could be

evaluated. The lowest frequency that can be measured by the impedance analyzer is 20

MHz. In many resistivity surveys, the measuring frequency can be much lower than 20

MHz. Therefore, the correlations at 1 KHz are also presented.

Figure 4.12 shows that the theoretical correlations between the volumetric water

content and effective electrical conductivity at both frequencies exhibit non-linear saddle-

like shapes. At high volumetric water contents, the mixture becomes more conductive

with the addition of more clay particles because of the high surface conductance of clay

particles. However, at low volumetric water contents, further addition of clay particles

will block the electrical current flow through the mixture because the solid phase of clay

particles is non-conductive. Thus mixture electrical conductivity decreases with

decreasing porosity at low volumetric water contents. At the same frequency and

volumetric water content, the effective electrical conductivity of a saturated bentonite and

sand mixture increases with increasing percentage of bentonite. A peak effective

electrical conductivity exists for each mixture and, the volumetric water content where

this peak occurs increases with increasing amount of bentonite. Almost all effective

electrical conductivities measured at 20 MHz by the impedance analyzer are satisfactorily

predicted by the theoretical correlations. The effective electrical conductivity at 1 kHz is

lower than that at 20 MHz because the contribution of the polarization loss to the

effective electrical conductivity increases with increasing frequency.

As previously discussed, the total specific surface area of a sand-bentonite mixture is

largely determined by the percentage of bentonite. Therefore, the theoretical correlations

in Figure 4.12 also reflect how the total specific surface area affects the correlation

between volumetric water content and effective electrical conductivity of a soil when the

pore fluid DC electrical conductivity is low. The application of these theoretical

correlations for natural soils and for soils with different pore fluid DC electrical

conductivities need to be further studied.
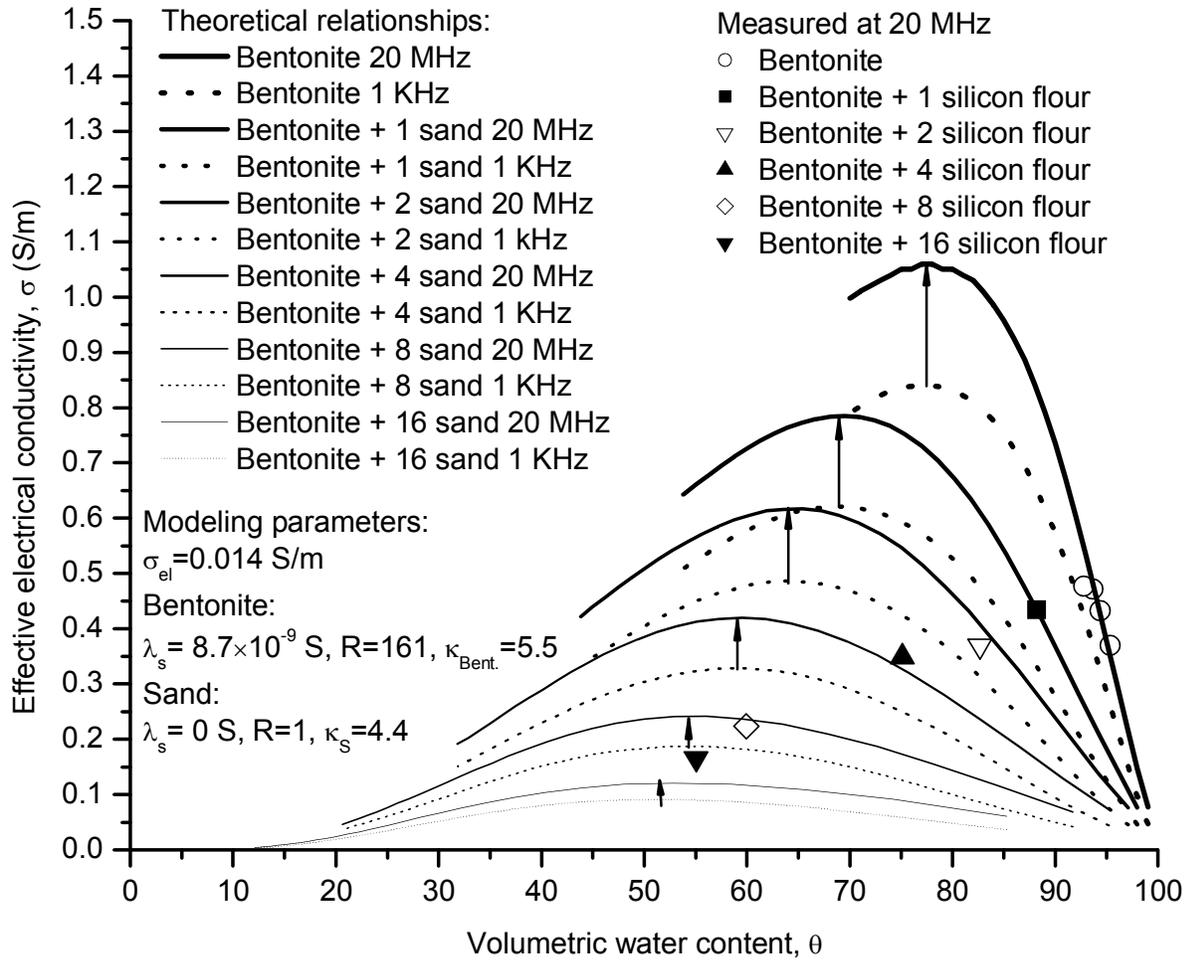
Figure 4.12 Relationship between effective electrical conductivity and volumetric water content of bentonite-silicon flour mixtures

4.5 Conclusions

To order to relate the frequency-dependent electromagnetic property of clayey soils to their composition and structure, a physically-based model is presented which can quantitatively evaluate the influences of a variety of compositional and structural factors on soil dielectric spectra, including volumetric water content, anisotropy, clay percentage, clay mineralogy, clay surface conductance, pore fluid chemistry and state of flocculation and dispersion. The effects of the above factors on the dielectric spectra of saturated

bentonite, kaolinite and bentonite-sand mixtures are analyzed. Several conclusions are drawn from the analysis:

(1) At frequencies less than 50 MHz, the real permittivity of a soil decreases with increasing pore fluid DC electrical conductivity; at frequencies higher than 50 MHz, the influences of pore fluid DC electrical conductivity on soil real permittivity become small.

(2) Anisotropy has a bigger impact on the DC electrical conductivity of a soil than on its real permittivity.

(3) The real permittivity of a soil increases and its electrical conductivity decrease with increasing flocculation. The effects of increasing flocculation on the dielectric spectrum of a soil tend to cancel the effects of increasing pore fluid DC electrical conductivity.

(4) The real permittivity at 1 GHz is primarily determined by the volumetric water content. For a specific soil, the higher the volumetric water content, the higher the real permittivity at 1 GHz.

(5) The dielectric dispersion magnitude from 50 MHz to 1 GHz is primarily controlled by the clay mineralogy and clay percentage, which may be conclusively characterized by the total specific surface area of a soil. At the same volumetric water content, a high specific surface area corresponds a higher dielectric dispersion magnitude from 50 MHz to 1 GHz.

(6) A peak effective electrical conductivity exists for soils containing bentonite when the pore fluid electrical conductivity is low; the volumetric water content at which this peak occurs increases with increasing amount of bentonite.

Three theoretical correlations are established: (1) correlations between volumetric water content and real permittivity 1 GHz; (2) correlations between volumetric water content and dielectric dispersion magnitude from 50 MHz to 1 GHz; (3) correlations between volumetric water content and the effective electrical conductivity at 1 kHz and 20 MHz. These correlations are validated by the experimental data of the saturated sand, kaolinite, bentonite and mixtures of bentonite and silicon flours. A simple method is proposed to determine the total specific surface area and volumetric water content of sand, silt, pure clay and mixtures of pure clay and sand.

Good matches between the predicted and measured dielectric spectra of different soils demonstrate the usefulness of the theoretical model in relating the soil electromagnetic properties to their components and structure. The model can also be very useful for studying the electromagnetic properties of other mixtures where anisotropic or isotropic inclusions of various shapes are distributed in a conductive medium.